CHEMICAL ENGINEERING TRANSACTIONS
VOL. 127, 2026
A publication of AIDIC
The Italian Association of Chemical Engineering
Online at www.cetjournal.it
Guest Editors: Laura Capelli, Marzio Invernizzi, Selena Sironi

ISBN 979-12-81206-28-1; **ISSN** 2283-9216
DOI: 10.3303/CET26127055

Green Hydrogen Production via Anion Exchange Membrane Water Electrolysis: A Critical Review

Cesar A. Rodriguez Aburto[a], Roberto E. Solís Farfán[a], Jesús V. Vara Sánchez[a], Jorge A. Montaño Pisfil[a], Pablo M. Morcillo Valdivia[a], Alex A. Vallejos Zuta[a], César A. Santos Mejía[a], Juan T. Medina Collana[b,*]

[a]Facultad de Ingenieria Electrica y electronica, Universidad Nacional del Callao Bellavista Callao, Perú
[b]Facultad de Ingenieria Quimica, Universidad Nacional del Callao, Bellavista 07011, Perú
jtmedinac@unac.edu.pe

Anion-exchange membrane water electrolysis (AEMWE) has emerged as one of the most promising technologies for green hydrogen production, as it does not require platinum group metals (PGMs) and operates under alkaline conditions using abundant and cost-effective transition metal catalysts. However, the gap between performance demonstrated at the laboratory scale and requirements for industrial-scale deployment remains. This review takes an integrated approach to the main factors influencing this transition: the kinetics of hydrogen evolution (HER) and oxygen evolution (OER) reactions in an alkaline medium, the system operating parameters, and the state of the art in PGM-free electrocatalysts and anion exchange membranes. The analysis reveals that OER is the primary kinetic limiting factor, that no commercial membrane simultaneously meets all established performance criteria, and that the joint selection of the membrane–catalyst pair is the most critical design criterion for system optimization. Recent advances in both components establish AEMWE as a viable technology for sustainable hydrogen production at industrial scale.

1. Introduction

Growing concern over greenhouse gas emissions resulting from the intensive use of fossil fuels has driven the search for clean energy sources in sectors such as transportation and industry (Mustapha et al., 2025). In this context, hydrogen is positioned as a priority alternative for decarbonization; however, 95 % of global hydrogen production is obtained through fossil-fuel-based reforming, with associated emissions of 1.3 Gt of CO_2 annually (Yang et al., 2025). Faced with this paradox, more than 50 countries have opted for water electrolysis coupled with renewable energy, with global demand for hydrogen projected to grow by 20 % to 40 % by 2030 (Mustapha et al., 2025). To meet this demand, four main technologies have been developed: alkaline water electrolysis (AWE), proton exchange membrane electrolysis (PEMWE), AEMWE, and solid oxide electrolysis cells (SOEC) (Medina Collana et al., 2025); the comparative characteristics of AWE, PEMWE, and AEMWE are summarized in Table 1. AWE is the most cost-effective and commercially mature technology, although the low activity of its electrodes limits its efficiency; PEMWE achieves higher efficiency and high hydrogen purity, although its economic viability is constrained by its dependence on PGMs such as iridium and platinum; whereas SOEC achieves the highest energy efficiency, although it requires temperatures above 700 °C, which limit its practical applicability (Zhang et al., 2025). Given these limitations, AEMWE emerges as the most promising alternative by combining AWE's affordability and compatibility with non-precious catalysts with the zero-gap configuration, where electrodes directly contact the membrane, and the operational efficiency of PEMWE (Kim et al., 2025). Its operation with dilute alkaline electrolytes reduces the system's corrosiveness, and its high dynamic response makes it particularly compatible with intermittent renewable sources (Zhang et al., 2025). However, several challenges still hinder its industrial transition: the lower mobility of OH^- ions limits ionic conductivity (Guo et al., 2026), while the intrinsic slowness of the OER and the susceptibility of membranes and catalysts to chemical degradation constitute the main outstanding issues (Zheng et al., 2025). This review provides a comprehensive analysis of the electrochemical principles of AEMWE, its key operating parameters, and the state of the art in

Paper Received: 11 May 2026; Revised: 8 July 2026; Accepted: 17 July 2026
Please cite this article as: Rodriguez Aburto C.A., Solís Farfán R.E., Vara Sánchez J.V., Montaño Pisfil J.A., Morcillo Valdivia P.M., Vallejos Zuta A.A., Santos Mejía C.A., Medina Collana J.T., 2026, Green Hydrogen Production via Anion Exchange Membrane Water Electrolysis: A Critical Review, Chemical Engineering Transactions, 127, 325-330 DOI:10.3303/CET26127055

PGM-free electrocatalysts and anion exchange membranes, with the aim of identifying the most promising strategies for accelerating its transition to industrial scale.

Table 1: Comparison of the main operational characteristics of AWE, PEMWE, and AEMWE

Parameter	AWE	PEMWE	AEMWE	Reference
Electrolyte	25–40 wt% KOH	Water	KOH/Water	(Lei et al., 2024)
Cell temperature (°C)	70–90	50–80	60–80	(Mustapha et al., 2025)
Cell pressure (MPa)	<3.0	<5.0	<3.5	(Mustapha et al., 2025)
Typical anode catalyst	Ni/Co/Fe-based	IrO_2/RuO_2	PGM-free	(Lei et al., 2024)
Typical cathode catalyst	Ni/C-Pt	Pt/C	Ni/Co-based	(Lei et al., 2024)
Membrane	Asbestos	Nafion	AEM	(Lei et al., 2024)
Current density (A cm^{-2})	<0.8	>1	>1	(Yang et al., 2025)
Cell voltage (V)	1.5–2.6	1.4–2.3	1.8–2.2	(Lei et al., 2024)
Power consumption (kWh Nm^{-3})	4.0–5.47	4.53–6.1	4.2–5.5	(Mustapha et al., 2025)
Operational flexibility (%)	10–100	0–100	0–100	(Mustapha et al., 2025)
H_2 purity (%)	≥99.5	≥99.9	≥99.9	(Yang et al., 2025)
Lifetime (h)	60,000	100,000	30,000	(Tang et al., 2025)
Electrolyzer efficiency (%)	59–70	65–82	60–75	(Tang et al., 2025)
Technology status	Mature	Commercial	Laboratory	(Yang et al., 2025)

2. Electrochemical principles of the AEMWE

In the AEMWE, the cathode reduces water, releasing H_2 and OH^- ions, which migrate through the anion exchange membrane (AEM) to the anode, where they are oxidized to produce O_2 and water (Zheng et al., 2025). The system thus involves two complementary half-reactions: the HER at the cathode (Eq. 1) and the OER at the anode (Eq. 2), yielding the overall reaction ($2H_2O \rightarrow 2H_2 + O_2$, $\Delta E° = 1.23$ V).

$$\text{Cathode (HER): } 4H_2O + 4e^- \rightarrow 2H_2 + 4OH^- \quad E° = -0.828 \text{ V (pH=14)} \tag{1}$$

$$\text{Anode (OER): } 4OH^- \rightarrow O_2 + 2H_2O + 4e^- \quad E° = +0.401 \text{ V (pH=14)} \tag{2}$$

However, the operating voltage exceeds the thermodynamic threshold of 1.23 V ($\Delta G° \approx 237.2$ kJ mol^{-1}, 25 °C, 0.1 MPa) due to ohmic losses, parasitic resistances, and slow kinetics of both half-reactions (Zheng et al., 2025), whose overpotentials account for 30–40 % of the total losses (Muhyuddin et al., 2025). Under alkaline conditions, HER requires H–OH bond dissociation as a preliminary step, representing an inherent kinetic barrier (Kim et al., 2025), and proceeds via two alternative routes, both initiated by the Volmer step (Eq. 3):

$$\text{Volmer: } H_2O + e^- \rightarrow H^* + OH^- \tag{3}$$

$$\text{Heyrovsky: } H^* + H_2O + e^- \rightarrow H_2 + OH^- \tag{4}$$

$$\text{Tafel: } H^* + H^* \rightarrow H_2 \tag{5}$$

In the Volmer–Heyrovsky pathway, adsorbed H* reacts with a water molecule (Eq. 4), whereas in the Volmer–Tafel pathway, two adsorbed H* species recombine directly (Eq. 5). The rate-limiting step depends on H* adsorption strength: weak binding limits the Volmer step while strong binding limits the desorption steps (Muhyuddin et al., 2025). The anodic OER requires four electron transfers to generate O_2 (Zheng et al., 2025) and can proceed via the adsorbate evolution mechanism (M–OH, M–O, M–OOH) or the lattice oxygen mechanism (LOM), which directly involves lattice oxygen in O–O bond formation, albeit with a higher risk of structural instability (Kim et al., 2025). Regardless of the mechanism, scaling relationships among intermediates impose a minimum overpotential of ~370 mV (Zheng et al., 2025), positioning OER as the step that most severely limits the kinetic performance of AEMWE.

3. AEMWE configuration

The AEMWE operates using individual cells stacked in series, each consisting of flow field plates that house the membrane-electrode assembly (MEA) in a zero-gap configuration, comprising gas diffusion layers (GDL), catalytic layers (CL), and the central AEM (Yang et al., 2025), as illustrated in Figure 1. In the typical configuration, KOH/H_2O is fed on the cathode side, where OH^- migrates through the AEM toward the anode, producing O_2 and regenerating water.

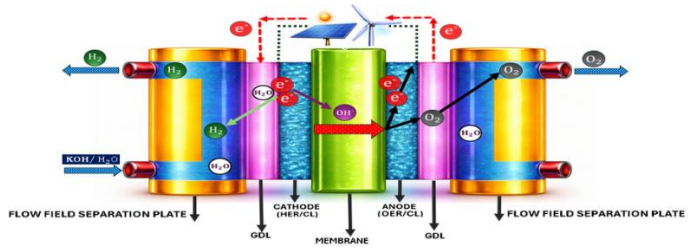

Figure 1: Schematic of a single AEMWE cell

4. Operating parameters for AEMWE electrolyzers

4.1 Operating temperature and pressure

Most conventional AEMWE systems operate between 60 and 80 °C (Mustapha et al., 2025). Within this range, higher temperatures make the electrolytic process more energetically favorable and kinetically active, simultaneously enhancing ion transport and water mobility at the membrane level (Yassin et al., 2026); however, exceeding 80 °C compromises the integrity of quaternary ammonium groups, affecting membrane conductivity and operational life (Wijaya et al., 2024). The first high-temperature cell (HT-AEMWE), operated at 110 °C with PGM-free catalysts, showed that heating from 50 to 95 °C raised ionic conductivity from 119 to 216 mS cm^{-1}, exceeded 5 A cm^{-2} below 2.2 V, and degraded only 4 μV h^{-1} after 500 h at 1.0 A cm^{-2} (Yassin et al., 2026). Regarding pressure, these systems operate at up to 3.5 MPa (Mustapha et al., 2025), and anion-exchange membranes keep H_2/O_2 crossover below 1 % under pressure differences of up to 3.0 MPa between electrodes (Yang et al., 2025); above 5.0 MPa, however, crossover becomes critical, compromising system safety (Wijaya et al., 2024) and hindering water transport, which increases polarization losses (Yang et al., 2025). Clamping pressure during MEA assembly is equally important, as ~0.5 MPa effectively reduces ohmic and interfacial losses (Wijaya et al., 2024). Next-generation electrolyzers are projected to operate above 7.0 MPa, placing additional demands on mechanical and chemical resistance of membranes (Muhyuddin et al., 2025).

4.2 Electrolyte feed

Generally, an alkaline solution is used, typically KOH at concentrations of 0.1 to 1 M, or 1 wt% K_2CO_3 (Muhyuddin et al., 2025). Hyter, an Italian manufacturer of AEMWE electrolyzers, uses KOH at concentrations of 3 to 5 M, which reduces resistive losses and improves efficiency (Mustapha et al., 2025). Pure water is the most sustainable option, although its low ionic conductivity limits performance; recent advances address this by incorporating TiO_2 nanoparticles into the catalytic layers, generating local basicity (pH ~14) and achieving 3.0 A cm^{-2} at 2.08 V with ~1,400 h of stability (Guo et al., 2026). In contrast, Cl^- in seawater promotes the competing chlorine evolution reaction (ClER), while Mg^{2+}/Ca^{2+} induce scaling, limiting AEMWE selectivity and stability.

5. Anion exchange membranes

AEM plays a major role in the overall performance of the electrolyzer: it transports OH^- ions from cathode to anode and physically separates H_2 and O_2 in each half-cell. Structurally, it combines a polymeric backbone providing mechanical support and chemical resistance with cationic functional groups responsible for ionic conduction, making it a decisive system component (Lu et al., 2025). Both components present interrelated challenges: increasing functional group density improves ionic conductivity but causes excessive swelling, loss of structural integrity, and intensifies polymer chain exposure to OH^-, accelerating chemical degradation and reducing the membrane's alkaline stability (Wijaya et al., 2024). Polymers based on poly (arylene ether) proved unsuitable for long-term operation due to the vulnerability of their ether bonds to OH^- (Lu et al., 2025). Consequently, fully ether-free polyarylene structures have been developed, combining better chemical resistance with mechanical properties, with the backbone choice being a fundamental design variable (Ng et al., 2023). Functional groups present a similar problem: quaternary ammonium groups, the most commonly used, are susceptible to degradation via nucleophilic substitution (SN1/SN2) and Hofmann elimination driven by OH^- (Lu et al., 2025). In contrast, the 1,2,4,5-tetramethylimidazole group in Sustainion® X37-50, by blocking all OH^- attack sites, confers greater alkaline stability (Ng et al., 2023). Table 2 compares commercially available AEMs, highlighting their strengths and limitations. Their performance depends on both intrinsic membrane properties and catalyst compatibility, making the membrane–catalyst pair decisive for system optimization (Ng et al., 2023). Additionally, anionic ionomers in the MEA catalytic layers ensure catalyst dispersion and local ionic conduction (Mustapha et al., 2025). Despite recent advances, no commercial membrane simultaneously satisfies all target performance criteria, indicating opportunities for further materials development.

Table 2: Major commercial AEM membranes for water electrolysis

Brand (Company)	Product	Strength / Challenge	Reference
Fumasep® (Fumatech)	FAA-3 series	Affordable, widely benchmarked; hydroxide attack rapidly depletes ion-exchange capacity and conductivity	Wijaya et al., 2024
Sustainion® (Dioxide Materials)	X37-50	High performance, energy efficiency, ionic conductivity; polystyrene-based backbone fractures when dry	Ng et al., 2023
PiperION® (Versogen)	PiperION	Stiff, water-repellent chain lacks ether links; highly ion-conductive, fuel-cell promising; needs longer-term testing	Ng et al., 2023
Aemion™ (Ionomr Innovations)	AF1-HNN8, AF1-HNN5	Phenyl ring improves resistance to OH^-, wide pH range; high ionic conductivity may cause gas, liquid crossover	Altinisik et al., 2026
Orion TM1 (Orion Polymer)	TM1	Free of ether groups; minimal loss of ionic capacity after 1,000 h; hydroxide exposure erodes polymer over time	Altinisik et al., 2026

6. PGM-free electrocatalysts for AEMWE

6.1 Catalysts for the hydrogen evolution reaction

In alkaline media, HER requires an additional water-dissociation step versus acidic media, requiring electrocatalysts balancing H adsorption, O–H cleavage, and OH^- desorption (Kim et al., 2025); per the Sabatier principle, efficiency is achieved when the free energy of H* adsorption nears zero (Muhyuddin et al., 2025). Unlike powdered electrodes, self-supporting electrodes have gained prominence by eliminating binders and improving adhesion and gas transport at high current densities (Yang et al., 2025). Zhao et al. (2023) demonstrated distinct roles in B,V-Ni_2P: V reduces the water dissociation barrier to 0.43 eV, further lowered to 0.36 eV by B,V co-doping, while synergy balances H* adsorption/desorption, reaching 1 A cm^{-2} at 1.92 V. Xie et al. (2024) developed a 3D WS_2 superstructure operating at 1.70 V and 1 A cm^{-2}, attributed to stepped defects optimizing H* adsorption and a hydrophilic surface accelerating bubble release. Dong et al. (2025) reported the self-supporting Int-Ni/MoO_2 electrode, whose MoO_2 nanoparticle interlayer forms a homostructural interface enhancing mechanical adhesion and mitigating bubble impact, achieving 7.57 A cm^{-2} at 2.0 V, establishing self-supporting electrodes as a promising strategy for industrial-scale AEMWE. Among these, Int-Ni/MoO_2 leads in both current density and stability, whereas B,V-Ni_2P and WS_2 remain limited to lower densities and higher degradation rates, leaving stack-level validation the most pressing gap toward industrial deployment.

6.2 Catalysts for the oxygen evolution reaction

OER is the kinetically limiting step, requiring higher overpotentials and stricter stability due to its multi-electron, thermodynamically complex nature (Mirizzi et al., 2025). A key trend in PGM-free OER catalysts is in situ surface reconstruction into active oxyhydroxide phases such as NiOOH and FeOOH, for which synthesis strategies have been developed to maximize this transformation (Wang et al., 2025). Seijas et al. (2025) synthesized NiFe-LDH via mild homogeneous alkalization, obtaining a nanostructured material with high defect density and cationic Fe clustering that, per in situ analysis and first-principles calculations, reduces the OER energy barrier and maximizes conversion to the active phase, reaching 1 A cm^{-2} at 1.69 V. Mirizzi et al. (2025) prepared amorphous $Ni_{0.75}Fe_{0.25}O$ via cost-effective sol-gel synthesis and, used as an anode, achieved 3.7 A cm^{-2} at 2.0 V, attributing performance to high Ni^{3+} (NiOOH) content, which activates Ni sites for charge transfer during OER. Kim et al. (2026) identified W_1-NiFeOOH via machine learning screening as one of the highest-performing PGM-free OER catalysts reported; W acts as a subsurface modulator altering electron density in Ni-O-Fe bridges, stabilizing the γ-NiOOH phase and achieving 13.1 A cm^{-2} at 2.0 V, establishing AI-assisted design as an emerging strategy for OER discovery. Among these, W_1-NiFeOOH attains the highest current density with 500 h stability at the industrially relevant 1 A cm^{-2}, whereas NiFe-LDH and $Ni_{0.75}Fe_{0.25}O$ remain confined to 100 h, leaving validation beyond 500 h the most pressing overall gap and constraining their readiness for scale-up.

6.3 Bifunctional catalysts

Using a single material for HER and OER simplifies MEA fabrication and reduces costs, although reconciling the electronic requirements of both reactions remains challenging due to different pathways. Jiang et al. (2024) activated 304 stainless steel, SS304(SM-CA), via etching and electrochemical treatment, generating dual-active LDH phases in situ and achieving 1.95 V at 1 A cm^{-2}. Similarly, Min et al. (2025) developed V-Ni_3S_2-P/NF nanorods on Ni foam, reaching 1.626 V at 1 A cm^{-2} and outperforming the Pt/C‖RuO_2 benchmark. Despite these advances, SS304(SM-CA) offers longer stability at lower cost, whereas V-Ni_3S_2-P/NF achieves lower voltage but only short-term validation, and the HER/OER trade-off common to both complicates catalyst design. Table 3 compares representative PGM-free AEMWE catalysts and their strengths and remaining challenges.

Table 3: PGM-free electrocatalysts for AEMWE (1 M KOH; n.r. = not reported; n.d. = not detected)

Catalyst (Reaction)	J (A cm^{-2}) @ V (V)	Temp. (°C)	Stability h@A cm^{-2} (Degradation mV h^{-1})	Strength / Challenge	Ref
B,V-Ni_2P (HER)	1.0@1.92	55	100@0.5 (<0.50)	V dopant lowers water-dissociation barrier; complex three-step synthesis required	(Zhao et al., 2023)
WS_2 3D[a] (HER)	1.0@1.70	60	1,000@1.0 (0.0097)	Flexible 3D structure resists mechanical wear; underperforms Pt/C at low densities	(Xie et al., 2024)
Ni_4Mo–MoOx/GDL (HER)	3.0@2.03	80	100@3.0 (n.r.)	Oxide-alloy cooperation speeds Volmer step; ionomer optimization still needed	(Serban et al., 2025)
Int-Ni/MoO_2 (HER)	7.57@2.0	60	1,000@1.0 (0.0040)	Interlayer dissipates bubble shock, securing catalyst; Mo dissolution persists	(Dong et al., 2025)
NiFe-LDH (RT) (OER)	1.0@1.69	70	100@1.0 (0.41)	Fe-clustering minimizes OER energy barrier; Fe leaching degrades performance	(Seijas et al., 2025)
(Ni,Fe)S_2@Ti_3C_2 (OER)	2.0@1.75	70	500@0.5 (20[b])	Ti3C2 support triggers LOM pathway, boosting activity; complex multi-step synthesis	(Wang et al., 2025)
$Ni_{0.75}Fe_{0.25}O$ (OER)	3.7@2.0	80	~100@1.0 (n.d.)	Lowest overpotential among Ni/Fe ratios; performance sensitive to binder formulation	(Mirizzi et al., 2025)
W_1-NiFeOOH (OER)	13.1@2.0	80	500@1.0[c] (n.r.)	Lower overpotential than Ir-based catalyst; W raw material costs exceed Ni, Fe	(Kim et al., 2026)
SS304 (SM-CA) (BI)	1.0@1.95	60	250@1.0 (n.r.)	Low-cost steel matches Pt/C, exceeds IrO_2 performance; used inactive counter electrode	(Jiang et al., 2024)
V-Ni_3S_2-P/NF (BI)	1.0@1.626	80	100@1.0 (n.r.)	Lower full-cell voltage than Pt/C‖RuO_2 at all tested J; stability assessed short-term only	(Min et al., 2025)

[a] 30 wt% KOH. [b] Unit: μA cm^{-2} h^{-1}. [c] Stability at 60 °C; maximum J at 80 °C; BI: Bifunctional

7. Conclusions

AEMWE represents a promising technology for the sustainable production of green hydrogen, combining the advantages of alkaline and proton-exchange membrane electrolysis. The AEM is the key component, simultaneously governing ionic conductivity, gas separation, and chemical stability of the system. Despite significant progress in ether-free polymer backbones and more robust functional groups, no commercial membrane yet satisfies all established performance requirements. In this context, the membrane–catalyst pair emerges as the primary design criterion for system optimization. Recent advances in noble-metal-free electrocatalysts have enabled high current densities (>7.5 A cm^{-2} at 2.0 V) and extended HER stability (>1,000 h), while operation with pure water has approached ~1,400 h of durability, demonstrating the technological potential of AEMWE systems. Nevertheless, ensuring the durability of all components under real-world operating conditions remains the primary barrier to industrial deployment. Closing these gaps will require standardized stack-scale testing protocols and extended durability studies across catalyst categories. The integrated development of membrane materials, electrocatalysts, and MEA architectures is therefore essential to ensure efficiency and scalability, enabling AEMWE to become a central technology in the green hydrogen economy.

References

Altinisik H., Celebi C., Ozden A., Devrim Y., Ozgur Colpan C., 2026, A review on membranes for anion exchange membrane water electrolyzers, Renewable and Sustainable Energy Reviews, 226, 116277.

Dong A., Lin G., Li Z., Wu W., Cao X., Li W., Wang L., Zhao Y., Chen D., Sun L., 2025, Interlayer-bonded Ni/MoO2 electrocatalyst for efficient hydrogen evolution reaction with stability over 6000 h at 1000 mA cm−2, Nature Communications, 16(1), 4955.

Guo J., Wang R., Yang Y., Zhang Q., Cao F., Zhao J., Pan C., Ling T., 2026, Local alkalinity enables high-performance pure water anion exchange membrane electrolysis, Nature Communications, 17(1), 2335.

Jiang T., Zouridi L., Li N., Binas V., Stuart M.C.A., Aravind P.V., Jayawardhana B., Pescarmona P.P., Kyriakou V., 2024, Activation of low-cost stainless-steel electrodes for efficient and stable anion-exchange membrane water electrolysis, Journal of Materials Chemistry A, 12(43), 29909–29922.

Kim J.H., Jo H.J., Han S.M., Kim Y.J., Kim S.Y., 2025, Recent advances in electrocatalysts for anion exchange membrane water electrolysis: design strategies and characterization approaches, Energy Materials, 5(8), 500099.

Kim J., Kwon I.S., Lim J., Lee S.A., Cheon W.S., Cho J.H., Park S.H., Kim Y.J., Lee M.G., Kwon K.C., Park S.H., Kim S.Y., Jang H.W., 2026, Machine-learning-guided tungsten single atoms promote oxyhydroxides for noble-metal-free water electrolysis, Nature Communications, 17(1), 2344.

Lei J., Wang Z., Zhang Y., Ju M., Fei H., Wang S., Fu C., Yuan X., Fu Q., Farid M.U., Kong H., An A.K., Deng R., Liu F., Wang J., 2024, Understanding and resolving the heterogeneous degradation of anion exchange membrane water electrolysis for large-scale hydrogen production, Carbon Neutrality, 3(1), 25.

Lu Q., Yan X., Guo W., Li G., Wang J., Jiang N., Wang X., Ba T., Liu P., Zhou J., Wang J., Hu L., Zhou T., Huang R., Hu B., Zhang K., Ren Z., 2025, Research progress on alkaline anion exchange membranes (AEMs) for the application of hydrogen production by water electrolysis, Nano Research, 18(3), 94907252.

Medina Collana J.T., Carrasco-Venegas L., Ancieta-Dextre C., Rodriguez-Taranco O., Gabriel-Hurtado D., Montaño-Pisfil J., Rodriguez-Aburto C., Chávez-Sánchez W., Santos-Mejía C., Morcillo-Valdivia P., Herrera-Espinoza N., 2025, Analysis of the main hydrogen production technologies, Sustainability, 17(18), 8367.

Min K., Kang S., Lee E., Ham H.C., Baeck S.H., 2025, Unveiling the role of V and P dual-doping in Ni3S2 nanorods: enhancing bifunctional electrocatalytic activities for anion exchange membrane water electrolysis, Small Structures, 6(9), 2500217.

Mirizzi L., Muhyuddin M., Lo Vecchio C., Mosca E., Baglio V., Gatto I., Berretti E., Lavacchi A., Valerio C., Ficca C.A., Viscardi R., Nisticò R., Santoro C., 2025, Amorphous nanostructured Ni–Fe oxide as a notably active and low-cost oxygen evolution reaction electrocatalyst for anion exchange membrane water electrolysis, Industrial Chemistry & Materials, 3(4), 485–497.

Muhyuddin M., Santoro C., Osmieri L., Ficca V.C.A., Friedman A., Yassin K., Pagot G., Negro E., Konovalova A., Lindquist G., Twight L., Kwak M., Berretti E., Di Noto V., Jaouen F., Elbaz L., Dekel D.R., Mustarelli P., Boettcher S.W., Lavacchi A., Atanassov P., 2025, Anion-exchange-membrane electrolysis with alkali-free water feed, Chemical Reviews, 125(15), 6906–6976.

Mustapha F., Guilbert D., Gross B., 2025, Advancements in anion exchange membrane electrolysers: from catalysts to life cycle assessment, International Journal of Sustainable Energy, 44(1), 2520812.

Ng W.K., Wong W.Y., Rosli N.A.H., Loh K.S., 2023, Commercial anion exchange membranes (AEMs) for fuel cell and water electrolyzer applications: performance, durability, and materials advancement, Separations, 10(8), 424.

Seijas-Da Silva A., Hartert A., Oestreicher V., Romero J., Jaramillo-Hernández C., Muris L.J.J., Thorez G., Vieira B.J.C., Ducourthial G., Fiocco A., Legendre S., Huck-Iriart C., Mizrahi M., López-Alcalá D., Freiberg A.T.S., Mayrhofer K.J.J., Waerenborgh J.C., Baldoví J.J., Cherevko S., Varela M., Thiele S., Lloret V., Abellán G., 2025, Scalable synthesis of NiFe-layered double hydroxide for efficient anion exchange membrane electrolysis, Nature Communications, 16(1), 6138.

Serban A., Liu M.T., Chen N., Chen H.M., Hu X., 2025, An oxide-promoted, self-supported Ni4Mo catalyst for high current density anion exchange membrane water electrolysis, Energy & Environmental Science, 18(3), 1533–1543.

Tang Z., Wu B., Yan K., Luo J., Haq M.U., Zeng L., 2025, Long-term stability for anion exchange membrane water electrolysis: recent development and future perspectives, Future Batteries, 5, 100024.

Wang J., Liu Y., Yang G., Jiao Y., Dong Y., Tian C., Yan H., Fu H., 2025, MXene-assisted NiFe sulfides for high-performance anion exchange membrane seawater electrolysis, Nature Communications, 16(1), 1319.

Wijaya G.H.A., Im K.S., Nam S.Y., 2024, Advancements in commercial anion exchange membranes: a review of membrane properties in water electrolysis applications, Desalination and Water Treatment, 320, 100605.

Xie L., Wang L., Liu X., Chen J., Wen X., Zhao W., Liu S., Zhao Q., 2024, Flexible tungsten disulfide superstructure engineering for efficient alkaline hydrogen evolution in anion exchange membrane water electrolysers, Nature Communications, 15(1), 5702.

Yang L., Dong S., Yang T., Liu J., Liu S., Wang K., Wang E., Wang H., Chou K.-C., Hou X., 2025, Membrane electrode assembly design for high-efficiency anion exchange membrane water electrolysis, Research, 8, 0907.

Yassin K., Baranov A.A., Zhong J., Dekel D.R., 2026, High-temperature anion exchange membrane water electrolysis, ACS Energy Letters, 11(2), 2257–2264.

Zhang L., Qi F., Ren R., Gu Y., Gao J., Liang Y., Wang Y., Zhu H., Kong X., Zhang Q., Zhang J., Wu L., 2025, Recent advances in green hydrogen production by electrolyzing water with anion-exchange membrane, Research, 8, 0677.

Zhao T., Wang S., Jia C., Rong C., Su Z., Dastafkan K., Zhang Q., Zhao C., 2023, Cooperative boron and vanadium doping of nickel phosphides for hydrogen evolution in alkaline and anion exchange membrane water/seawater electrolyzers, Small, 19(27), 2208076.

Zheng Z., Deng L., Xing G., Peng S., Chen S., Lv C., 2025, Progress and perspectives on NiFe layered double hydroxide catalysts for the alkaline oxygen evolution reaction, eChem, 1(1), 3.